sciendo

B&H Electrical Engineering, Volume 17, Issue 2, 2023:24-31
ISSN:2566-3143, eISSN:2566-3151, DOI: 10.2478/bhee-2023-0009

Original scientific paper

Submitted: September 19, 2023

Accepted: October 24, 2023

POWER TRANSFORMER NUMERICAL MODELING TO LOCATE PARTIAL DISCHARGE SOURCE USING THE UHF TECHNIQUE

Đorđe Dukanac[1,2]

Abstract: Using three-dimensional full-wave electromagnetic simulations with Ansys HFSS, this paper analyses the effect of the actual design of a small power transformer on the propagation of ultra-high frequency (UHF) waves from a partial discharge (PD) source to four UHF antennas. Based on these results, the goal is to localize the source of PD. Three power transformer models of different complexity are used to do that. Due to the effects of their all taken into account reflections and diffractions caused by the metal parts in the power transformer, the received PD waveforms at UHF sensors are distorted to an appropriate extent. Time differences of arrivals (TDOAs) of the signals at pairs of four simulated UHF sensors are investigated to estimate the location of the PD source. The benefits of this assessment of the PD source location using this simulation software are analysed.

Keywords: electromagnetic (EM) wave, localization, model, partial discharge (PD), power transformer, signal delay, time difference of arrival (TDOA), ultra-high frequency (UHF) antenna

INTRODUCTION

The most important interpretation of Maxwell's equations is that they assume that electromagnetic (EM) waves propagate in the absence of any charges or currents. Initially, EM waves require time-dependent charges or currents to be produced, but once generated, they propagate without the need for additional charges or currents [1]. As shown in Figure 1, the changes in the electric field $\vec{E}_y$ are indicated by red arrows, and the changes in the magnetic field $\vec{B}_z$ are indicated by green arrows. These changes travel through space as an EM wave along the x axis from the current source to the receiving antenna.

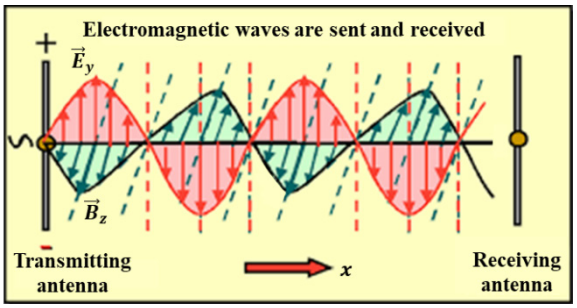


Figure 1: The propagation process of a cross-connected electric and magnetic field

Partial discharge (PD) detection by finding the released energy in the form of EM waves during PDs using an ultra-high frequency (UHF) antenna is one of the methods for determining the level of quality of the insulation system of power devices [2, 3]. The main advantage of the UHF PD detection system using an antenna is the possibility of finding the PD signal without first turning off the power apparatus [4].

For a linear, isotropic, and homogeneous dielectric, the wave equations for a point source of spherical waves are [1]:

$$\frac{1}{v^2}\cdot\frac{\partial^2\vec{E}}{\partial t^2}-\frac{1}{r}\cdot\nabla^2\vec{E}=0 \quad (1)$$

$$\frac{1}{v^2}\cdot\frac{\partial^2\vec{B}}{\partial t^2}-\frac{1}{r}\cdot\nabla^2\vec{B}=0 \quad (2)$$

where: $\vec{E}$ is the electric field vector, $\vec{B}$ is the magnetic field vector, v is the phase velocity of the wave, r is the distance from a point source, t is time.

For materials with relative permittivity ε_r and relative permeability μ_r, the phase velocity of waves v is given by:

$$v=\frac{c}{\sqrt{\mu_r\varepsilon_r}} \quad (3)$$

where c is the propagation speed of the EM wave in a vacuum.

The Ansys HFSS (High-Frequency Structure Simulator) simulation software utilizes adaptive meshing. The initial mesh is created, fields are solved, and then the mesh is refined based on high concentration and/or gradient areas.

The difference between every two adaptive passes is ΔS. To ensure simulation accuracy, Ansys HFSS makes adaptive

[1] Joint Stock Company "Elektromreža Srbije", Serbia
[2] Correspondence email: djordje.dukanac@ems.rs
© 2023 Author(s). This is an open access article licensed under the Creative Commons Attribution License 4.0. (http://creativecommons.org/licenses/by/4.0/).

passes until ΔS threshold is met. This code solves Maxwell's equations in terms of the S-matrix, which represents the percentages of transmitted or reflected power [5].

High-voltage (HV) insulation is the most important part of HV equipment used in the electric power system. The main function of electrical insulation is to withstand high electric fields between phases or between the phase and the neutral conductor.

When an electric field exceeds a certain level, PDs can occur due to areas of enhanced field, such as gas cavities or metal protrusions. The appearance of PDs in the electrical insulation can indicate the aging of the insulation and, in the long run, further reduce the insulation integrity, leading to equipment failure [6]. Finding PDs at an early stage is necessary to prevent the failure of HV equipment.

Power apparatus is generally in the form of metal-enclosed equipment. PDs release energy such as light, heat, and EM waves, which are blocked by the metal case and require internal sensors for detection.

The power transformer consists of different materials that can be [7]:

1) dielectric (e.g., mineral oil, oil-paper insulation, pressboard),
2) electrically conductive (e.g., copper),
3) soft magnetic (e.g., electrical steel).

Active metal parts of the power transformer can affect the shape and magnitude of the received signals at UHF sensors, the source of which is a PD in the insulation of the power transformer. At the same time, the attenuation and distortion of the signal at the receiving UHF antenna are all the greater if the PD signal path is more distorted in relation to the straight line that connects the PD source and the corresponding UHF sensor.

According to [8], the radiated field amplitude has a linear relationship with the PD current pulse's amplitude and exponentially decreases with an increase in pulse width.

[9] explains how to use two, three, or four UHF sensors to locate PD in a simplified model of a power transformer using simulations in MATLAB. This is done under several fundamental presumptions, such as the presence of white Gaussian noise, the dielectric permittivity of the mineral oil, the average signals' attenuation in the oil, and suitable delayed PD source voltage signals with two possible assumed limiting forms. In [10], a simplified power transformer model in CST Microwave Studio software was used with five electric field probes to achieve the true PD position.

In [11], it is proposed a method that is based on the TDOA database to solve the problem of PD source location, which does not have the non-convergence problem. .NET Windows Presentation Foundation (.NET WPF) and Helix 3D were used to model the transformer structure with simplified obstacles. It was concluded that to achieve even better location accuracy, the tested UHF sensors should be installed as far as possible in the direction of three axes.

A method for locating PD sources based on the idea of time reversal is provided in [12]. For a more thorough evaluation of the method's performance on a real transformer and in the presence of noise, additional theoretical and experimental studies are required.

In [13] and [14], the placement of a PD source in a 180 MVA and 200 MVA three-phase transformer, respectively, was simulated using four electric field sensors, a binary particle swarm optimization method, and a finite integration technique (FIT). A 3D simulation model of a 630 kVA distribution transformer was created in [15] using the same software. The simulated EM waveforms, their propagation periods, cumulative energies, and voltage signal amplitudes, as a function of UHF sensor position, therefore showed a fair agreement with those obtained by experiment and theory. In [16], the CST Microwave Studio software was used to create a computer model of a 300 MVA power transformer. This model was then used to calculate the attenuation of the PD signal and, using that information, determine the best locations for the UHF sensors.

In this paper, using simulations in Ansys HFSS software, the location of the PD source in a 5 MVA three-phase transformer was determined by analysing the PD voltage signals received by the UHF sensors using the first peak detection method.

Four equations with four unknown variables (i.e., x_l, y_l, z_l, T_1) [9] have been used to pinpoint the location of the PD source when four UHF sensors are employed:

$$v_u \cdot T_1 = \sqrt{(x_l - x_1)^2 + (y_l - y_1)^2 + (z_l - z_1)^2} \quad (4)$$

$$v_u \cdot T_2 = \sqrt{(x_l - x_2)^2 + (y_l - y_2)^2 + (z_l - z_2)^2} \quad (5)$$

$$v_u \cdot T_3 = \sqrt{(x_l - x_3)^2 + (y_l - y_3)^2 + (z_l - z_3)^2} \quad (6)$$

$$v_u \cdot T_4 = \sqrt{(x_l - x_4)^2 + (y_l - y_4)^2 + (z_l - z_4)^2} \quad (7)$$

where: $T_2 = T_1 + t_{21}$, $T_3 = T_1 + t_{31}$, $T_4 = T_1 + t_{41}$; $v_u = 20.23$ cm/ns is the speed of the UHF signal in mineral oil; x_l, y_l, z_l are the coordinates of the PD source I; x_k, y_k, z_k are the coordinates of the UHF sensor k (k=1,2,3,4); T_1 is the time of arrival (TOA) of the PD signal from the source I to the reference sensor D_1; t_{21}, t_{31}, t_{41} are the TDOAs between the PD signals at the sensors D_2, D_3, D_4 and the reference sensor D_1, respectively.

B&H Electrical Engineering, Volume 17, Issue 2, 2023:24-31
ISSN:2566-3143, eISSN:2566-3151, DOI: 10.2478/bhee-2023-0009

all four UHF sensors are significantly different from the corresponding preceding peaks for all three power transformer models and the specific PD pulse mentioned in the first section. The differences in the times of the first peaks of the signal pairs at sensors 2, 3, 4 and the reference sensor 1 give the TDOAs t_{21}, t_{31}, t_{41} respectively, between those signal pairs. In addition, the coordinates of the UHF sensors are known in advance.

This paper is organized as follows. The first section contains descriptions of three models of power transformers of varying complexity from simplified to composite. The simulation results of both PD signal propagation and PD source localization are presented in the second section. The third section discusses another example of PD source location and compares it to the first example. The final section provides the main conclusion.

1. MODELS OF PD SOURCE, UHF SENSORS, AND POWER TRANSFORMER

For successful simulations of signal propagations from a PD source through the structure of a power transformer for receiving such signals at UHF sensors, it is necessary to properly model the transmitting and receiving antenna, as well as the construction of the power transformer.

1.1. Model of transmitting and receiving antenna

Figure 2 shows the dipole antenna used in the computer simulation for the PD source and the UHF antennas. The arms of the antenna have dimensions of 60 mm x 5 mm and are made of copper.



Figure 2: Dipole antenna with dimensions of 124 mm x 5 mm [17]

Figure 3a) shows the considered dipole antenna, whose radiation is limited by a cube with 500 mm edges, in order to test the total gain of the antenna. The dipole antenna's central point is located precisely at a distance of 250 millimetres from the origin of the Cartesian coordinate system in all three dimensions (x, y, and z). Figure 3b) shows the polar diagram of the total gain of a dipole UHF antenna expressed in decibels [dB], at a frequency of 1 GHz, for the position of the antenna in Figure 3a).

It is evident from Figure 3b) that the radiation pattern of the transmitting dipole antenna is not omnidirectional. In the x-y plane, the radiation intensity is lowest along the longitudinal axis of the UHF transmitting antenna and within ±15° of its centre. Also, the radiation intensity is weaker along the vertical z-axis of antenna symmetry. The radiation pattern is three-dimensional and appears more cubic than spherical in shape. Similarly, when receiving UHF signals, the antenna's ability to pick up radiated power varies depending on the direction.

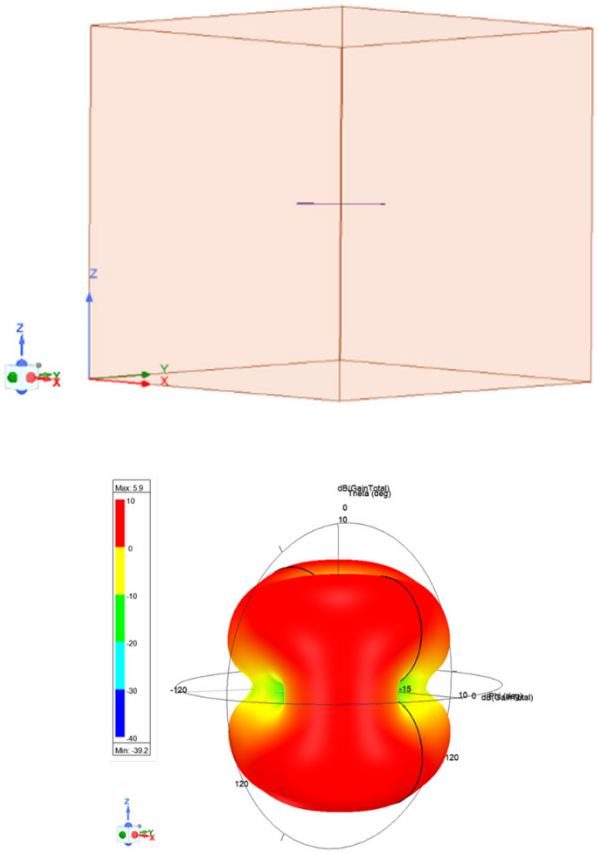


Figure 3: a) Dipole UHF antenna positioned in the centre of the cube. b) Correspondent polar diagram of the total gain of the antenna expressed in decibels [dB] [17]

1.2. Descriptions of power transformer simulation models of different complexity

A small 5 MVA three-phase power transformer with a transmission ratio of 66/11 kV was taken into consideration. The transformer tank measures 2300 mm (L) x 880 mm (W) x 2800 mm (H) [17].

To analyse the influence of the actual construction of the power transformer, we will look at examples of UHF signal propagation from the PD source to the receiving UHF antennas for the following cases:

1) for an empty transformer tank made of stainless steel 304 and filled with transformer mineral oil;
2) for a transformer tank made of stainless steel 304 filled with transformer mineral oil containing a three-limb magnetic core;
3) for a typical construction of a power transformer consisting of a) 304 stainless steel transformer tank filled with insulating mineral oil, b) three-limb, four-

stage (with 7 degrees) magnetic core, and c) three-phase low-voltage (LV) and HV copper windings.

The following are the adopted locations (centres of symmetry) for receiving UHF antennas (UHF sensors): $D_1[65,65,2750]\ mm$, $D_2[1150,440,2758]\ mm$, $D_3[2235,815,2755]\ mm$, and $D_4[70,810,2760]\ mm$.

It is assumed that the PD source is located at the point: $I[248,498,675]\ mm$. Located in the lower part of the third phase of the winding, it can be found near the front right oblique side of the core's third limb. It is positioned amidst the 5th and 6th discs of the LV winding.

1.3. Limitations of the typical power transformer simulation model

Three-phase LV and HV windings have to be simplified due to the computer's and simulation software's restricted capabilities.

The paper insulation of the windings is impregnated with oil, which reduces its dielectric strength. Therefore, the insulation of the three-phase windings is considered to have the dielectric strength of mineral oil. The LV and HV windings consist of 42 discs that are of corresponding sizes. The intermediate insulation between adjacent windings of LV and HV disks in the radial direction,1.2 mm thick, could not be taken into account. It is considered to be copper. Each HV disk is divided into two parts along the vertical axis with a 1.2 mm gap instead of the original four parts. The signal attenuation is a little bit higher if the two gaps of 1.2 mm each are disregarded. For an EM wave with a wavelength of 20.23 cm in mineral oil (dielectric constant 2.2) and a wave frequency of 1 GHz, a 1.2 mm aperture is tiny. Due to wave diffraction at such a small aperture, the power of the signal beam through such an opening is scattered in many directions concerning the opening itself, which is why the power of that beam weakens in the direction of the shortest feasible distance to the UHF sensor.

Since the insulating layers of the pressboard are also impregnated with oil, which reduces the dielectric strength of the pressboard, it is assumed that the intermediate insulation of the pressboard between the LV and HV windings has the dielectric strength of mineral oil.

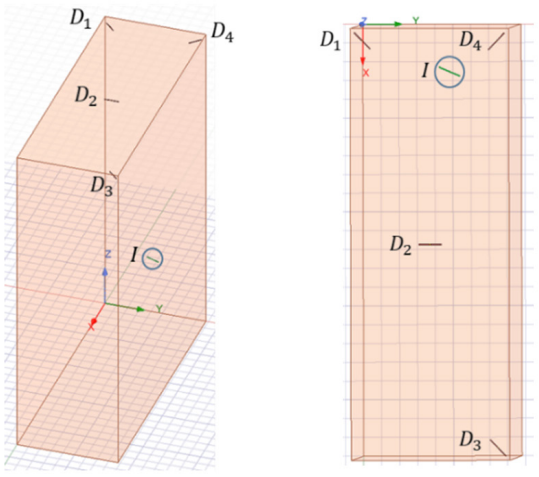
The main reasons for the mentioned limitations of the transformer windings are, first of all, the limited possibilities of random-access memory (RAM) for storing data that are simultaneously processed, then the processor (i.e., data processing speed), and, finally, the complexity of the simulation software Ansys HFSS itself in the computer. The HV winding model grows noticeably more complex as the number of its sections rises, which causes the problems outlined above.

In a material with a 2.2 dielectric constant, EM waves propagate at a speed of 0.2023 m/s. The longest feasible distance in the tank is 3728.86 mm, and the correspondent EM wave delay is 18.644 ns. However, the distances between the UHF sensors and the PD source are typically substantially shorter. The broadband pulse of the PD source has an amplitude of 1 V, a minimum frequency of 0 Hz, and a maximum frequency of 1 GHz.

2. SIMULATION RESULTS OF PD SIGNALS' PROPAGATIONS AND PD SOURCE LOCATION

For the specified placement of the PD source and positioning of four UHF sensors close to the top wall of the transformer tank and observed from the front and top:

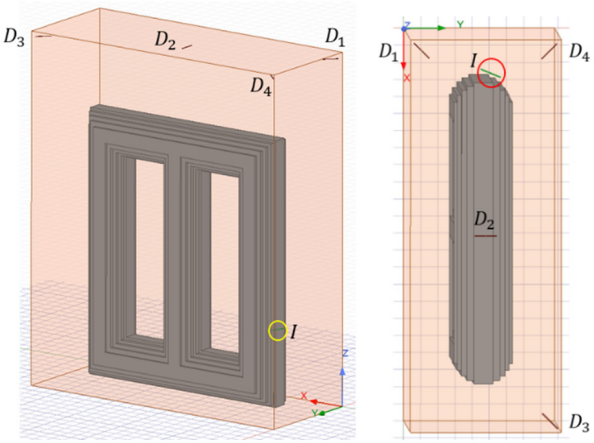
- Figure 4a)–b) illustrates a simplified model of a power transformer, which consists of a stainless steel 304 tank filled with insulating mineral oil;
- Figure 5a)–b) depicts a more complex model of a power transformer made up of a three-limb magnetic core made of electrical steel and a 304 stainless steel tank filled with insulating mineral oil;
- A typical power transformer is depicted in Figure 6 a)–b) as having a three-limb core made of electrical steel, three-phase LV and HV copper windings, and a tank made of 304 stainless steel filled with insulating mineral oil.



a) b)

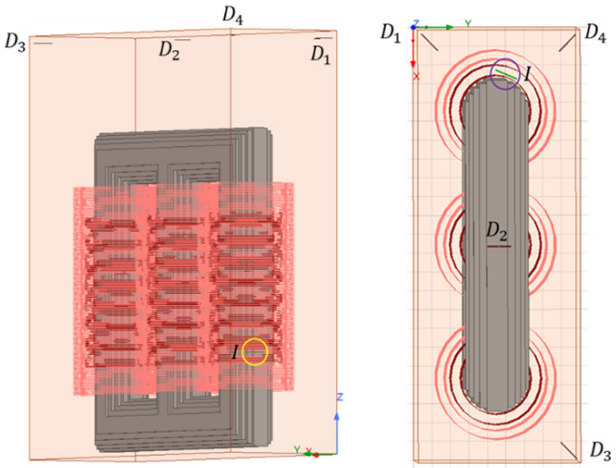
Figure 4: A simplified model of the power transformer in a) front view and b) top view

B&H Electrical Engineering, Volume 17, Issue 2, 2023:24-31
ISSN:2566-3143, eISSN:2566-3151, DOI: 10.2478/bhee-2023-0009



a) b)

Figure 5: A more complex model of the power transformer in a) front view and b) top view



a) b)

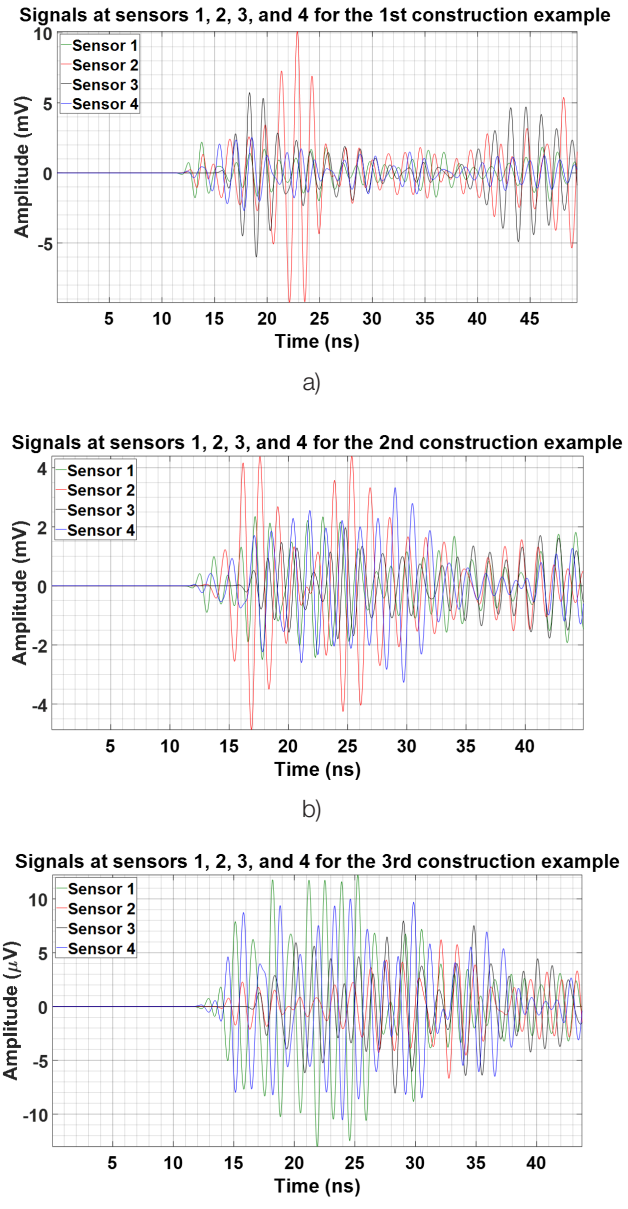
Figure 6: A typical model of the power transformer in a) front view and b) top view

The PD signals at the corresponding UHF sensors are shown combined in various colours (green for D_1, red for D_2, black for D_3, and blue for D_4) in the following Figure 7a)–c) for each of the three power transformer models discussed above.

The following can be deduced from the initial packets of signal waveforms at UHF sensors 1–4 lasting around 10 ns, which are predominantly caused by direct propagation of waves from the PD source I:

- When the three-limb magnetic core is not present, Figure 7b) shows a decline in amplitude (i.e., attenuation) by 3.65 times of the recorded signal at UHF sensor 3 highlighted with a black curve;
- In Figure 7c), you can notice significant attenuations in the recorded signals' amplitudes, with UHF Sensor 1 experiencing the least attenuation (approximately 169 times) and UHF Sensor 2 experiencing the most attenuation (about 2231 times), followed by UHF Sensor 3 at 930 times and UHF Sensor 4 at 287 times. These attenuations result from how the PD source is shaped and positioned between the fifth and sixth disks of the LV winding;
- As observed in Figure 7a)–c), the effects of diffraction around and reflection from distinct metal obstacles cause the forms of the amplitude envelopes of individual signals on UHF sensors to differ.

Only reflections off the tank walls and the power transformer's active components are responsible for the wave packets that come after the first in the recorded signals at UHF sensors 1–4.



a)

b)

c)

Figure 7: PD signals at sensors 1–4 for three different model types: a) a simplified model, b) a more complex model, and c) a common model

For three instances of power transformer construction, Table I displays the moments of the first peaks of the PD signals at UHF sensors 1–4.

Table I: Moments of the appearance of the first peaks of the PD signals at sensors 1–4 for three examples of power transformer construction

Construction	$t_1[ns]$	$t_2[ns]$	$t_3[ns]$	$t_4[ns]$
steel tank (α)	11.89	12.68	15.71	11.79
+core (β)	11.89	13.09	15.82	12.09
+windings (γ)	12.32	13.36	15.86	12.30

The results in Table I show that while the paths of the PD signals to sensors 2, 3, and 4 are lengthened and they arrive later by 0.41 ns, 0.11 ns, and 0.29 ns, respectively, the magnetic core almost has no effect on the path of the PD signal from the source to the UHF sensor 1. The three-phase copper windings and the three-limb magnetic core affect the signals' delays of (0.15–0.68) ns, depending on the position of the UHF sensor in relation to the state when the metal tank of the power transformer is empty. Sensor 2 has the longest delay (0.68 ns), whereas sensor 3 has the shortest delay (0.15 ns). For sensor 1 and sensor 4, the lag is 0.43 ns and 0.51 ns, respectively.

Table II shows the TDOAs of PD signals at UHF sensors 2–4 in relation to the signal at reference sensor 1 for the theoretical case and three examples of the power transformer construction.

Table II: Calculated TDOAs of the PD signals at the pairs of UHF sensors 1–4 for the theoretical (i.e., ideal) case and three examples of power transformer designs

Construction	$dt_{21}[ns]$	$dt_{31}[ns]$	$dt_{41}[ns]$
ideal case (ζ)	7.07E-10	3.79E-09	-5.87E-11
+ steel tank (α)	7.91E-10	3.82E-09	-9.89E-11
+ mag. core (β)	1.20E-09	3.93E-09	1.98E-10
+ windings (γ)	1.04E-09	3.54E-09	-1.85E-11

When the TDOAs for three transformer construction examples are compared to the TDOA in the ideal case in absolute values, it can be concluded that:

- $|dt_{31}|$ is up to 1.07 times deviated (i.e., is 1.07 times smaller for the third construction example),
- $|dt_{41}|$ is up to 3.37 times deviated (i.e., is 3.37 times larger for the second construction example),
- $|dt_{21}|$ is up to 1.7 times deviated (i.e., is 1.7 times larger for the second construction example).

In Table III, the mutual deviations of TDOAs of PD signals at the pairs of UHF sensors 1–4 and the mean values of their absolute values for the three considered simulated transformer construction cases in comparison with the theoretical case are given. Sensor serves as the reference sensor.

The mean deviation of the absolute values of TDOAs of the PD signals at the pairs of UHF sensors 1–4 from the ideal case is the greatest in the second simulated case and least in the first simulated case.

Table III: Mutual deviations of TDOAs of signals at pairs of sensors 1–4 and mean absolute values for three simulated instances in comparison to the ideal case

TDOAs errors	$D_2 - D_1$	$D_3 - D_1$	$D_4 - D_1$
$\Delta(dt_{\alpha,\zeta})[s]$	8.4E-11	2.9E-11	-4.0E-11
		5.1E-11	
$\Delta(dt_{\beta,\zeta})[s]$	5.0E-10	1.4E-10	2.6E-10
		3.0E-10	
$\Delta(dt_{\gamma,\zeta})[s]$	3.3E-10	-2.5E-10	4.0E-11
		2.1E-10	

Table IV presents the calculated locations of the PD source for the theoretical case and three examples of simulated structures of power transformers.

Table IV: Calculated positions of the PD sources for the theoretical case and three simulated examples

Construction	$x[m]$	$y[m]$	$z[m]$
ideal case (ζ)	2.48E-01	4.98E-01	6.75E-01
+ steel tank (α)	1.84E-01	5.27E-01	5.43E-01
+ mag. core (β)	1.58E-01	3.04E-01	5.52E-01
+ windings (γ)	1.70E-01	5.05E-01	8.17E-01

Table V shows mutual deviations in the calculated coordinates of the PD source and the mean value of their absolute values for the three considered simulated cases in relation to the theoretical (i.e., ideal) case.

Table V: Mutual deviations in the positions of the PD source along the axes and the mean value of their absolute values for 3 simulated cases in relation to the ideal case

TDOAs errors	x axis	y axis	z axis
$\Delta d_{\alpha,\zeta}[cm]$	-6.39E+00	2.88E+00	-1.32E+01
		7.49E+00	
$\Delta d_{\beta,\zeta}[cm]$	-9.05E+00	-1.94E+01	-1.23E+01
		1.36E+01	
$\Delta d_{\gamma,\zeta}[cm]$	-7.75E+00	7.15E-01	1.42E+01
		7.55E+00	

The mean value of the absolute values of the mutual deviations in the calculated positions of the PD source along the axes in relation to the ideal case is the greatest in the 2nd simulated case and the least in the 1st simulated case.

B&H Electrical Engineering, Volume 17, Issue 2, 2023:24-31
ISSN:2566-3143, eISSN:2566-3151, DOI: 10.2478/bhee-2023-0009

3. DISCUSSION

The different position I_1 of the PD source was taken into consideration in the article [17], as shown in Figure 8, which, when viewed from the front, is situated in the centre of the second phase of the three-phase copper windings on the right side of the middle limb of the electrical steel core beneath the top yoke. The PD source's real location in this case is I_1=[893.5,435,1118] mm. It is positioned against the 22nd disk of the LV winding and the bottom portion of the 22nd disk of the HV winding, closer to the LV winding. The mean value of the absolute deviations of the coordinates of the PD source in relation to the actual position in that situation, along with the arrangement of the UHF sensors, was 11.3 cm, which was the highest when accounting for the metal tank and the power transformer's three-limb core. The mean value of the absolute deviations of the coordinates of the PD source was 8.2 cm when the three-phase windings were also considered. The mean value of the absolute deviations of the coordinates of the PD source was 1.74 cm when just the metal tank of the power transformer was taken into account.

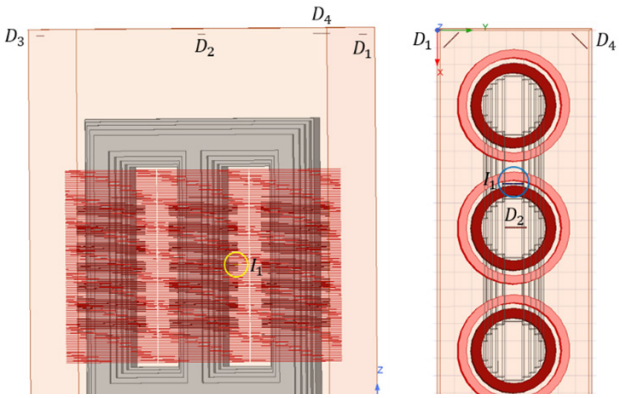


Figure 8: Composite model of the power transformer from the article [17] in a) front view and b) top view

In relation to the examples in the article [17], in the instances in this paper, the mean values of the absolute mutual deviations of the TDOAs of PD signals on pairs of UHF sensors 1–4 in the three examples of transformer construction compared to the ideal case are higher by 0.035 ns, 0.136 ns, and 0.131 ns, respectively. These three possibilities, which were earlier discussed, involve the effects of the tank, the tank and core, and the tank, core, and windings combined on the paths of signals' propagations from the PD source to the UHF sensors. In the example in this paper, the influence of the metal tank on the mean value of the absolute values of the coordinates of the PD source is 4.3 times greater.

It can be concluded that in both examples from Chapters 3 and 4, the magnetic core had a greater effect than the magnetic core and windings together in determining the location of the PD source, although, to a greater or lesser extent, the three-phase windings increased the delays of the UHF signals from the PD source to individual UHF sensors, depending on the size and number of metal obstacles in both examples.

4. CONCLUSION

The goal of this work was to find the location of the PD source and analyse the influence of the actual construction of the power transformer on the propagations of UHF EM waves from the PD source in the electrical insulation of the transformer winding to the UHF sensors.

Graphical displays of received PD signals at UHF sensors were made possible using simulations in Ansys HFSS, including the effects of all signals' reflections and diffractions due to the metal parts of the transformer on their paths from the PD source to the corresponding UHF sensors.

The flaw was that the PD source was represented by a UHF antenna rather than being point-like, which would have allowed it to radiate equally in all directions from the source. Due to the specific shape of the transmitting antenna and the absorption of reflected EM waves by the adjacent metal parts of the transformer near the antenna, this resulted in an uneven distribution of the radiation power around the antenna and an attenuation of the signal.

If not a single insulating distance between the LV and HV windings had been neglected, even though they were individually narrow for the unhindered passage of UHF waves, it is assumed that during waves' propagations, their joint action would have led to more regular shapes and larger amplitudes of the first signals' peaks. As a result, it would be easier to recognize first signals' peaks and more accurate to locate the PD source.

The magnitudes and ratios of TDOAs of PD signals at pairs of UHF sensors can affect the magnitudes and ratios of the results obtained for the PD source position, so when considering a transformer tank with a magnetic core and a magnetic core and copper windings together, sometimes the opposite results are obtained than expected.

To validate the results obtained through simulation, it would be useful to analyse the model of the transformer currently in use at the facility. The fixed positioning of UHF sensors and the inability to place the PD source in the desired location would pose a challenge, unlike the ease of accomplishing the same in simulations.

REFERENCES

[1] D. Fleisch, A Student's Guide to Maxwell's Equations (Student's Guides). UK: Cambridge University Press, 2008

[2] Đ. Dukanac, "Detection and analysis of a partial discharge signal in the power transformer using UHF method (in Serbian)," Energy, economy, ecology, No. 1–2, Year XXII, 2020, pp. 96–101, doi: 10.46793/EEE20-1-2.096D

[3] D. Dukanac, "Extraction of partial discharge signal in predominant VHF range in the presence of strong noise in power transformer," Electrical Engineering, Volume 105, Issue 5, 2023, pp. 3001–3018, doi: 10.1007/s00202-023-01855-x

[4] N. D. Roslizan, M. N. K. H. Rohani, A. S. Rosmi, B. Ismail, M. A. Jamlos, W. C. Leong, C. M. N. C. Isa, M. A. A. Jalil, "Comparison Study of UHF Sensor Modelling Based on 4th Order Hilbert Fractal Category for Partial Discharge Detection in Power Transformer," in Proc. IEEE 8th Conference on Systems Process and Control (ICSPC), Melaka, Malaysia, 2020, pp. 196–201, doi: 10.1109/ICSPC50992.2020.9305753

[5] Electronic design automation software, user's guide – High Frequency Structure Simulator. Pittsburgh, USA: ANSOFT CORPORATION, 2005

[6] V. A. Thiviyanathan, P. J. Ker, Y. S. Leong, F. Abdullah, A. Ismail, Md. Z. Jamaludin, "Power transformer insulation system: A review on the reactions fault detection challenges and future prospects," Alexandria Engineering Journal, Vol. 61, Issue 10, 2022, pp. 7697–7713, doi: 10.1016/j.aej. 2022.01.026

[7] M. J. Heathcote, The J & P Transformer Book. England: Newnes, 1998

[8] J. Du, W. Chen, B. Xie "Simulation Analysis on the Propagation Characteristics of Electromagnetic Wave Generated by Partial Discharges in the Power Transformer," in Proc. IEEE Conference on Electrical Insulation and Dielectric Phenomena, Toronto, ON, Canada, 2016, pp. 1–4, doi: 10.1109/CEIDP.2016.7785485

[9] D. Dukanac, "Application of UHF Method for Partial Discharge Source Location in Power Transformers," IEEE Transactions on Dielectrics and Electrical Insulation, Volume: 25, Issue: 6, 2018, pp. 2266–2278, doi: 10.1109/TDEI.2018.006996

[10] D. Antony, P. Mishra, A. Todi, N. A. John, A. M. Patankar "Partial discharge localisation in transformers using UHF technique: non-iterative method," International Journal of Information Technology, Volume: 13, 2021, pp. 291–297, doi: 10.1007/s41870-020-00481-1.

[11] N. Xue, J. Yang, D. Shen, P. Xu, K. Yang, Z. Zhuo, L. Zhang, J. Zhang "The Location of Partial Discharge Sources inside Power Transformers Based on TDOA Database with UHF Sensors," IEEE Access, Volume 7, 2019, pp. 146732–146744, doi: 10.1109/ACCESS.2019.2945893

[12] H. Karami, M. Azadifar, A. Mostajabi, M. Rubinstein, H. Karami, G. B. Gharehpetian, F. Rachidi "Partial Discharge Localization Using Time Reversal: Application to Power Transformers" Sensors, 20(5), 1419, 2020, pp. 1–15, doi: 10.3390/s20051419

[13] L. A. M. M. Nobrega, E. G. Costa, A. J. R. Serres, G. V. R. Xavier, M. V. D. Aquino "UHF Partial Discharge Location in Power Transformers via Solution of the Maxwell Equations in a Computational Environment," Sensors, Volume: 19, Issue: 15, 2019, pp. 1–13, 3435, doi: 10.3390/ s19153435

[14] H. R. Mirzaei, A. Akbari, E. Gockenbach, M. Zanjani, K. Miralikhani "A novel method for ultra-high-frequency partial discharge localization in power transformers using the particle swarm optimization algorithm," IEEE Electrical Insulation Magazine, Volume: 29, Issue: 2, 2013, pp. 26–39, doi: 10.1109/MEI.2013.6457597.

[15] T. Umemoto, S. Tenbohlen "Novel Simulation Technique of Electromagnetic Wave Propagation in the Ultra High Frequency Range within Power Transformers" Sensors, 18(12), 4236, 2018, pp. 1–16, doi: 10.3390/s18124236

[16] C. P. Beura, M. Beltle, S. Tenbohlen "Positioning of UHF PD Sensors on Power Transformers Based on the Attenuation of UHF Signals," IEEE Transactions on Power Delivery, Volume 34, No. 4, 2019, pp. 1520–1529, doi: 10.1007/s41870-020-00481-1

[17] Đ. Dukanac, "Analysis of the Influence of Active Parts of the Power Transformer on the Propagation of Signals from Source of Partial Discharges to UHF Sensors (in Serbian)," Energy, economy, ecology, No. 1, Year XXIV, 2022, pp. 74–80, doi: 10.46793/EEE22-1.74D

BIOGRAPHY

Đorđe Dukanac received the B.S., Magister, and Ph.D. degrees in electrical and computer engineering from the School of Electrical Engineering, University of Belgrade, Serbia, in 2005, 2016 and 2023, respectively. His primary research interests include UHF sensors, online PD monitoring, PD localization, and detection, extraction, and classification of UHF PD signals in power transformers.